Table V. Latent Heat Requirement for Acetone Distillation at 760 mmHg

acid concn, %	R_a change	heat required, kcal/kg (H_3PO_4 + H_2O)	av temp, °C	final acid concn, %
20.0	3 → 2	132	56	20.0
	2 → 1	132	58	20.0
	1 → 0	140	70	21.0
45.0	3 → 2	132	56	45.0
	2 → 1	133	59	45.1
	1 → 0	142	72	47.1
70.0	3 → 2	132	56	70.0
	2 → 1	136	60	70.6
	1 → 0	150	80	72.9
80.0	3 → 2	133	56	80.0
	2 → 1	140	61	80.6
	1 → 0	174	87	82.9

lution phase then were calculated from deviations from Raoult's Law by eq 7, where P^0 (mmHg) is the vapor pressure of the

$$\gamma_a = P_a/(x_a P_a^0) \qquad \gamma_w = P_w/(x_w P_w^0) \tag{7}$$

pure component at a given temperature, which is obtained from recent data (*11*, *12*). The activity coefficients of acetone (γ_a) is always larger than unity, except at very high acid concentration and very low values of R_a; it becomes quite large at low acid concentration and low R_a. This high activity coefficient of acetone is expected because of its low boiling point compared with that of water in phosphoric acid. However, the low γ_a value at high acid concentration with small amounts of acetone indicates the relative difficulty of complete distillation of acetone from the concentrated acid because it may form a relatively strong bond between acetone and phosphoric acid molecules. When the solution contained a large quantity of acetone, the γ_a value converged to a value of ~2.5 for all acid concentrations. The activity coefficient of water is usually less than 0.5 and decreases slightly as R_a decreases and as the acid concentration increases. These values of γ_a also indicate the preferential distillation of acetone from the solution since acetone has a larger activity coefficient than water. Figure 7 shows the activity coefficients of acetone and water at 70 °C, and similar patterns are predicted at other temperatures.

The overall latent heat requirements for the distillation of acetone from phosphoric acid of different concentrations are calculated from the ΔH values from eq 4 or a combination of eq 5 and 6 (Table V). The heat of vaporization for the solution at large R_a values is approximately the same as the heat of vaporization of pure acetone (7.64 kcal/(mol of acetone)), regardless of the phosphoric acid concentration, since most of the distillate is acetone, as indicated by Figure 5. The heat of vaporization gradually increases as R_a decreases and phosphoric acid concentration increases. The average boiling points of the solutions, within the R_a range listed, increase with the increase of phosphoric acid concentration.

Literature Cited

(1) Slack, A. V., Ed. "Phosphoric Acid"; Marcel Dekker: New York, 1968; Vol. 1, Part II.
(2) Kim, Y. K.; Walters, H. K., Jr.; Hatfield, J. D. *J. Agric. Food Chem.* **1974**, *22*, 1099-106.
(3) Walters, H. K., Jr.; Kim, Y. K.; Hatfield, J. D. U.S. Patent 4 152 402, May 1, 1979.
(4) Brunjes, A. S.; Bogart, M. J. P. *Ind. Eng. Chem.* **1943**, *35*, 255-60.
(5) Davis, D. S. *Ind. Chem.* **1961**, *37*, 528.
(6) Petrova, L. N. *Khim. Tekhnol.* **1974**, 57-8.
(7) Rhim, J. N.; Park, S. S.; Lee, H. O. *Hwahak Konghak* **1974**, *12*, 179-87.
(8) Brown, E. H.; Whitt, C. D. *Ind. Eng. Chem.* **1952**, *44*, 615-8.
(9) Schmalz, E. O. *Z. Phys. Chem.* **1970**, *245*, 344-50.
(10) Barr, A. J.; Goodnight, J. H.; Sall, J. P.; Helwig, J. T. "A User's Guide to SAS 76"; SAS Institute, Inc.: Raleigh, NC, 1976.
(11) Scott, D. W.; Osborn, A. G. *J. Phys. Chem.* **1979**, *83*, 2714-23.
(12) Ambrose, D.; Sprake, C. H. S. Townsend, R. *J. Chem. Thermodyn.* **1974**, *6*, 693-700.

Received for review October 21, 1980. Accepted March 27, 1981.

Second Virial Coefficients of Propane–Isomeric Hexane Mixtures

Sun W. Chun,[†] **Webster B. Kay,*** **and Amyn S. Teja**[‡]
Department of Chemical Engineering, The Ohio State University, Columbus, Ohio 43210

The compressibilities of five isomeric hexanes (*n*-hexane, 2-methylpentane, 3-methylpentane, 2,2-dimethylbutane, and 2,3-dimethylbutane) as well as their mixtures with propane were measured between 369.7 and 508 K. Second virial coefficients were calculated from the compressibility measurements and are presented in this paper. The results agree with values calculated by using the Tsonopoulos–Pitzer–Curl correlation.

Introduction

The thermodynamic properties of nonideal gases and vapors may easily be calculated from a knowledge of the virial coefficients and their dependence on temperature. For calculations at low or moderate pressures, the effect of vapor-phase nonidealities can reliably be estimated by using only the second virial coefficient. The proper accounting of these nonidealities is of great importance in, for example, the correlation of vapor-liquid equilibria. An advantage of expressing gas-phase nonidealities by means of the virial equation is that there is a theoretical relationship between the virial coefficients and the intermolecular potential function. Thus the second virial coefficient provides a direct link between experimental measurements, on the one hand, and intermolecular forces, on the other.

The aims of this work were to obtain second virial coefficient data for binary mixtures of propane with the isomers of hexane, so that the effect of the shape of the molecules on intermolecular forces in mixtures could be studied, and also to see whether the currently available correlations for second virial coefficients are able to predict the effects of shape on the properties of mixtures.

Many correlations of second virial coefficients have appeared in the chemical engineering literature. Among the more recent ones are those of Tsonopoulos (*1*), Hayden and O'Connell (*2*),

---

[†] Present address: Pittsburgh Energy Technology Center, 4800 Forbes Avenue, Pittsburgh, PA 15213.
[‡] Present address: School of Chemical Engineering, Georgia Institute of Technology, Atlanta, GA 30332.

0021-9568/81/1726-0300$01.25/0

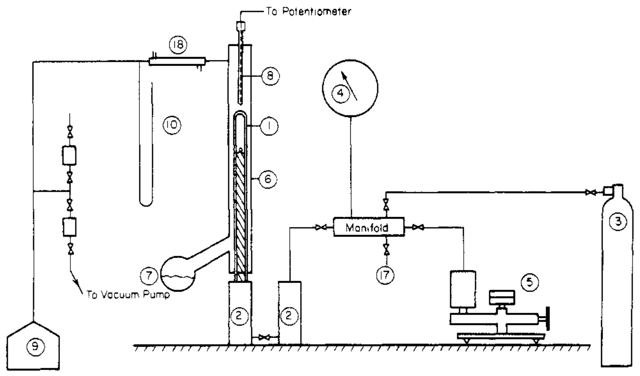

Figure 1. Schematic diagram of the apparatus.

and Tarakad and Danner (*3*). The Tsonopoulos-Pitzer-Curl correlation is among the more reliable ones for the hydrocarbons. This correlation was therefore chosen in our study of the effects of shape on the magnitude of the second virial coefficients.

Experimental Section

The apparatus and the experimental procedure for the determination of the isothermal compressibility of a sample were similar to those used in previous studies by Kay and Rambosek (*4*) and Jones and Kay (*5*). Figure 1 gives a schematic diagram of the apparatus.

The sample being studied was confined over mercury in the sealed end of sample tube 1. The tube was mounted in one leg of compressor block 2 which was connected to back leg 2 by stainless-steel tubing through a check valve. Pressure was transmitted to the sample through the mercury by admitting compressed nitrogen gas from cylinder 3. A dead weight gage (5) was used to measure the pressure in the system. The sample tube was surrounded by a double-walled jacket, to which was attached a side-arm boiling flask. A series of pure organic liquids were boiled in the flask, and the vapors were used to maintain the sample at a constant temperature. The temperature was controlled by varying the pressure of the vapor in the jacket. A thermocouple (8) placed just above the sample tube was used to measure the temperature. The volume of the sample was determined by measuring the length of the column of sample in the tube, the length having been related to the volume by a prior calibration.

The *P*-*V*-*T* data were obtained by setting a constant temperature and varying the pressure. Before each measurement, the sample was vigorously stirred with a steel ball by moving an external permanent magnet.

The dimensions of the experimental tube are shown in Figure 2. Further details of the experimental procedure and the loading of the tube are given elsewhere by Chun (*6*).

We estimate the precision of our pressure measurements to be ±0.0015 bar and the accuracy to be ±0.007 bar. For the temperature, the estimated precision is ±0.005 K, and the accuracy ±0.1 K. For the determination of the volume, a sensitive cathetometer reading to ±0.005 cm was used. This limited the precision of the volume measurements in the capillary to 0.25% and in the larger section of the tube to 0.05%. The compositions of the mixtures are estimated to be accurate to ±0.1%. The mass of the sample was determined from the *P*-*V*-*T* measurements of the superheated vapor. The results were adjusted so that the *Z* vs. 1/*V* curve extrapolated to unity at zero pressure. Further details of the calculation procedure can be found in the work by Jones and Kay (*5*).

The five research-grade isomeric hexanes were obtained from Phillips Petroleum Co., who furnished the following analysis of their purity with the most probable impurities given in parenthesis: *n*-hexane (methylcyclopentane) 99.96%; 2-methylpentane (3-methylpentane) 99.7%; 3-methylpentane (2-methylpentane) 99.83%; 2,2-dimethylbutane (2,3-dimethylbutane) 99.99%; 2,3-dimethylbutane (2,2-dimethylbutane) 99.81%. After percolation over silica gel, the samples were thoroughly degassed by a repeated freezing, pumping under

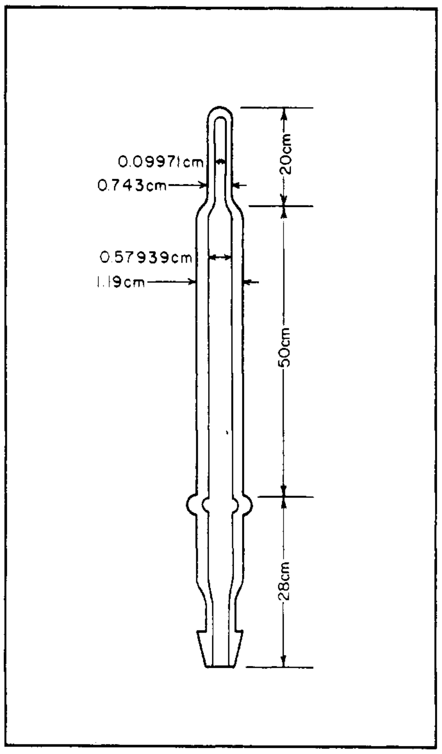

Figure 2. Dimensions of the experimental tube.

Table I. Second Virial Coefficients of Propane-*n*-Hexane Mixtures

T, K	*B*, m^3 $kmol^{-1}$	*T*, K	*B*, m^3 $kmol^{-1}$
x_1 = 0.0000			
373.15	−1.100	473.15	−0.555
393.15	−0.862	493.15	−0.524
426.15	−0.720	507.95	−0.469
453.15	−0.658		
x_1 = 0.1435			
373.15	−0.904	453.15	−0.576
393.15	−0.806	473.15	−0.502
413.15	−0.686	496.30	−0.432
426.15	−0.675		
x_1 = 0.1435			
373.15	−0.904	453.15	−0.576
393.15	−0.806	473.15	−0.502
413.15	−0.686	496.30	−0.432
426.15	−0.675		
x_1 = 0.4437			
373.15	−0.653	426.15	−0.461
393.15	−0.577	453.15	−0.383
413.15	−0.505	493.15	−0.309
x_1 = 0.6996			
373.15	−0.391	453.15	−0.235
393.15	−0.336	473.15	−0.210
413.15	−0.300	493.15	−0.190
426.15	−0.281	431.26	−0.271
x_1 = 0.8201			
373.15	−0.321	426.15	−0.224
393.15	−0.283	453.15	−0.194
413.15	−0.236	409.50	−0.258
x_1 = 0.9218			
373.15	−0.276	453.15	−0.162
393.15	−0.242	493.15	−0.134
413.15	−0.217	387.55	−0.254
426.15	−0.200		

Table II. Second Virial Coefficients of Propane–2-Methylpentane Mixtures

T, K	B, m^3 kmol^{-1}	T, K	B, m^3 kmol^{-1}
	$x_1 = 0.0000$		
383.15	−0.895	473.15	−0.520
403.15	−0.779	493.15	−0.474
426.15	−0.679	497.85	−0.459
453.15	−0.574		
	$x_1 = 0.1497$		
383.15	−0.754	473.15	−0.445
403.15	−0.677	493.15	−0.411
426.15	−0.588	486.49	−0.426
453.15	−0.499		
	$x_1 = 0.4446$		
383.15	−0.533	473.15	−0.316
403.15	−0.473	493.15	−0.280
426.15	−0.403	458.19	−0.328
453.15	−0.347		
	$x_1 = 0.6488$		
383.15	−0.400	473.15	−0.228
403.15	−0.357	493.15	−0.214
426.15	−0.304	431.97	−0.300
453.15	−0.257		
	$x_1 = 0.8196$		
403.15	−0.274	405.45	−0.253
426.15	−0.230		
	$x_1 = 0.9190$		
383.15	−0.266	473.15	−0.161
403.15	−0.236	493.15	−0.148
426.15	−0.210	386.58	−0.265
453.15	−0.175		

Table III. Second Virial Coefficients of Propane–3-Methylpentane Mixtures

T, K	B, m^3 kmol^{-1}	T, K	B, m^3 kmol^{-1}
	$x_1 = 0.0000$		
383.15	−0.926	473.15	−0.543
403.15	−0.819	493.15	−0.487
426.15	−0.691	504.62	−0.450
453.15	−0.592		
	$x_1 = 0.0000$		
383.15	−0.399	426.15	−0.309
403.15	−0.360	436.37	−0.290
	$x_1 = 0.1451$		
383.15	−0.792	473.15	−0.443
403.15	−0.665	493.15	−0.409
426.15	−0.578	492.65	−0.403
453.15	−0.499		
	$x_1 = 0.4453$		
383.15	−0.532	473.15	−0.313
403.15	−0.472	493.15	−0.284
426.15	−0.415	462.68	−0.331
453.15	−0.350		
	$x_1 = 0.8336$		
383.15	−0.311	473.15	−0.196
403.15	−0.282	493.15	−0.181
426.15	−0.244	404.92	−0.276
453.15	−0.211		
	$x_1 = 0.8850$		
383.15	−0.282	473.15	−0.172
403.15	−0.258	493.15	−0.161
426.15	−0.225	391.01	−0.268
453.15	−0.188		

vacuum, melting, and distilling cycle of operations. Research-grade propane with a purity of 99.99% was also provided by the Phillips Petroleum Co. It was degassed and packaged in sealed glass ampules ready for loading into the experimental tube. As a purity check, bubble- and dew-point pressures at constant temperature were determined for the pure isomeric hexane samples. If the pressures differed by more than 0.17 bar, the sample was discarded.

Table IV. Second Virial Coefficients of Propane–2,2-Dimethylbutane Mixtures

T, K	B, m^3 kmol^{-1}	T, K	B, m^3 kmol^{-1}
	$x_1 = 0.0000$		
383.15	−0.753	473.15	−0.479
403.15	−0.698	493.15	−0.424
426.15	−0.612	489.01	−0.440
453.15	−0.522		
	$x_1 = 0.1527$		
383.15	−0.674	473.15	−0.417
403.15	−0.594	493.15	−0.359
426.15	−0.508	477.91	−0.416
453.15	−0.464		
	$x_1 = 0.4490$		
383.15	−0.496	473.15	−0.296
403.15	−0.431	493.15	−0.272
426.15	−0.378	447.73	−0.336
453.15	−0.324		
	$x_1 = 0.6587$		
383.15	−0.392	473.15	−0.229
403.15	−0.348	493.15	−0.213
426.15	−0.310	425.36	−0.310
453.15	−0.259		
	$x_1 = 0.8205$		
383.15	−0.281	473.15	−0.170
403.15	−0.256	401.93	−0.254
426.15	−0.214		
	$x_1 = 0.9194$		
383.15	−0.245	426.15	−0.188
403.15	−0.219	385.15	−0.241

Table V. Second Virial Coefficients of Propane–2,3-Dimethylbutane Mixtures

T, K	B, m^3 kmol^{-1}	T, K	B, m^3 kmol^{-1}
	$x_1 = 0.0000$		
403.15	−0.827	473.15	−0.558
426.15	−0.725	493.15	−0.518
453.15	−0.617	500.23	−0.505
	$x_1 = 0.1516$		
383.15	−0.763	473.15	−0.467
403.15	−0.674	493.15	−0.429
426.15	−0.583	488.41	−0.435
453.15	−0.500		
	$x_1 = 0.4522$		
383.15	−0.527	473.15	−0.323
403.15	−0.470	493.15	−0.297
426.15	−0.404	459.36	−0.345
453.15	−0.353		
	$x_1 = 0.6508$		
383.15	−0.404	473.15	−0.253
403.15	−0.360	493.15	−0.225
426.15	−0.318	432.05	−0.307
453.15	−0.271		
	$x_1 = 0.9153$		
383.15	−0.281	473.15	−0.170
403.15	−0.258	493.15	−0.157
426.15	−0.222	387.50	−0.274
453.15	−0.189		

Results

Second virial coefficients for the five systems propane + *n*-hexane, propane + 2-methylpentane, propane + 3-methylpentane, propane + 2,2-dimethylbutane, and propane + 2,3-dimethylbutane are given in Tables I–V. Values of the second virial coefficient of *n*-hexane agree with values reported by McGlasham and Potter (*7*) within the experimental error. For the remaining isomeric hexanes, our data agree within experimental error with the data reported graphically by Griskey et al. (*8*).

Correlation of Second Virial Coefficients

We have compared our data with second virial coefficients predicted by the Tsonopoulous (*1*) modification of the Pitzer-Curl correlation. For nonpolar gases, the Tsonopoulos-Pitzer-Curl correlation is

$$BZ_c/V_c = f^{(0)} + \omega f^{(1)} \qquad (1)$$

where

$$f^{(0)} = 0.1445 - 0.330/T_R - 0.1385/T_R^2 - 0.0121/T_R^3 - 0.000607/T_R^8 \qquad (2)$$

$$f^{(1)} = 0.0637 + 0.331/T_R^2 - 0.423/T_R^3 - 0.008/T_R^8 \qquad (3)$$

and ω is Pitzer's acentric factor. The second virial coefficient B of any gas may thus be predicted from a knowledge of its critical properties and acentric factor.

The correlation may be extended to mixtures via the van der Waals one-fluid model whereby the pure-component properties T_c, V_c, Z_c, and ω are replaced by the pseudocritical values T_{cm}, V_{cm}, Z_{cm}, and ω_m as follows:

$$T_{cm}V_{cm} = \sum_i\sum_j x_ix_jT_{cij}V_{cij} \qquad (4)$$

$$V_{cm} = \sum_i\sum_j x_ix_jV_{cij} \qquad (5)$$

$$Z_{cm} = \sum_i x_iZ_{cii} \qquad (6)$$

$$\omega_m = \sum_i x_i\omega_i \qquad (7)$$

The van der Waals one-fluid model has been used with considerable success in extending equations of state to mixtures (see, for example, ref *9*). The like terms (i = j) are obtained from pure-component properties, whereas the unlike terms (i ≠ j) must be obtained from the properties of the binary mixtures. The usual prescription is to write

$$T_{cij} = \xi_{ij}(T_{cii}T_{cjj})^{1/2} \qquad (8)$$

$$T_{cij} = \{\tfrac{1}{2}(V_{cii}^{1/3} + V_{cjj}^{1/3})\}^3 \qquad (9)$$

where the binary interaction coefficient ξ_{ij} is obtained from binary-mixture properties. No further information is required to predict the properties of ternary and higher mixtures.

We have used the van der Waals one-fluid model together with the Lorentz-Berthelot mixture prescription (eq 8 and 9) and the Tsonopoulos-Pitzer-Curl equations to correlate second virial coefficients of the five propane-isomeric hexane systems. The results are summarized in Table VI. As can be seen, good agreement between prediction and experiment can be obtained with ξ_{ij} = 1.0 on all cases. On the whole, agreement appears to be within the experimental error of the data. It would therefore appear that the effect of size on the second virial coefficient is more important than the effect of the shape of the molecules and that this effect can be adequately represented by the Tsonopoulos-Pitzer-Curl equation and the van der Waals one-fluid model.

Table VI. Comparison of Calculated and Experimental Second Virial Coefficients of Propane-Isomeric Hexane Mixtures (ξ_{ij} = 1.0 Throughout)

system	no. of data	av abs deviation, %	max deviation, %
propane + *n*-hexane	40	5.0	11.7
propane + 2-methylpentane	38	2.7	7.3
propane + 3-methylpentane	39	2.4	6.5
propane + 2,2-dimethylbutane	37	3.7	10.8
propane + 2,3-dimethylbutane	34	4.9	9.6

Glossary

B	second virial coefficient
f	functions in eq 1
T	thermodynamic temperature
V	volume
x	mole fraction
Z	compressibility
ω	acentric factor
ξ	binary interaction coefficient

Subscripts

c	critical
i, j	components i and j
m	mixture value
R	reduced value

Literature Cited

(1) Tsonopoulos, Constantine *AIChE J.* **1974**, *20*, 263.
(2) Hayden, J. G.; O'Connel, J. P. *Ind. Eng. Chem. Process Des. Dev.* **1975**, *14*, 209.
(3) Tarakad, R. R.; Danner, R. P. *AIChE J.* **1977**, *23*, 685.
(4) Kay, W. B.; Rambosek, G. M. *Ind. Eng. Chem.* **1953**, *45*, 221.
(5) Jones, A. E.; Kay, W. B. *AIChE J.* **1967**, *13*, 717, 720.
(6) Chun, S. W. Ph.D. Thesis, The Ohio State University, Columbus, OH, 1964.
(7) McGlashan, M. L.; Potter, D. J. B., *Proc. R. Soc. London, Ser. A* **1962**, *267*, 478.
(8) Griskey, R. G.; Canjar, L. N.; Stuewe, C. W. *J. Chem. Eng. Data* **1963**, *8*, 341.
(9) Teja, A. S.; Patel, N. C.; Ng, N. H. *Chem. Eng. Sci.* **1978**, *33*, 623.

Received for review October 27, 1980. Accepted January 21, 1981.

Ternary Liquid–Liquid Equilibrium Data for the Cyclohexane–Cyclohexene–Ammonia System

Kiyoharu Ishida, Katsuji Noda,* and Osamu Morinaga
Department of Chemical Engineering, Shizuoka University, Hamamatsu 432, Japan

Ternary liquid–liquid equilibrium data for the cyclohexane–cyclohexene–ammonia system are measured at 0, 20, 30, and 40 °C and are correlated by the Othmer–Tobias and other plots.

Introduction

Liquid–liquid equilibrium data are useful for the design of liquid extraction processes and have been measured or correlated by many authors. Liquid ammonia has good solvency and se-

0021-9568/81/1726-0303$01.25/0